

Quantum dots confined in nanoporous alumina membranes

Jun Xu, Jianfeng Xia, and Jun Wang

Department of Materials Science and Engineering, Iowa State University, Ames, Iowa 50011

Joseph Shinar

Ames Laboratory-USDOE, Iowa State University, Ames, Iowa 50011

and Department of Physics and Astronomy, Iowa State University, Ames, Iowa 50011

Zhiqun Lin^{a)}

Department of Materials Science and Engineering, Iowa State University, Ames, Iowa 50011

(Received 27 March 2006; accepted 16 August 2006; published online 26 September 2006)

CdSe/ZnS core/shell quantum dots (QDs) were filled into porous alumina membranes (PAMs) by dip coating. The deposition of QDs induced changes in the refractive index of the PAMs. The amount of absorbed QDs was quantified by fitting the reflection and transmission spectra observed experimentally with one side open and freestanding (i.e., with two sides open) PAMs employed, respectively. The fluorescence of the QDs was found to be retained within the cylindrical nanopores of the PAMs. © 2006 American Institute of Physics. [DOI: 10.1063/1.2357877]

Porous alumina membrane (PAM) fabricated by two-step anodic oxidation of aluminum (Al) consists of highly ordered hexagonal arrays of straight, cylindrical nanopores.¹ Although PAM was extensively used as a template to synthesize one-dimensional nanostructures with functional electronic characteristics, e.g., nanowires,² it has only recently been employed to control optical properties of colloid particles³ and conjugated polymers⁴ and to detect biomolecular binding⁵ by monitoring the absorption, emission, and reflectivity spectra. The large surface area of the PAM associated with the nanoporous structure facilitates a substantial change in refractive index upon the deposition of the molecules.

Quantum dots (QDs) are highly emissive, spherical nanoparticles with a few nanometers in diameter. They provide a functional platform for a class of materials for use in light emitting diodes,⁶ photovoltaic cells,⁷ and biosensors.⁸ Due to the quantum-confined nature of QDs such as cadmium selenide (CdSe), the variation of particle size provides continuous and predictable changes in fluorescence emission. By passivating most of the vacancies and trap sites on the CdSe surface with a higher band gap material such as zinc sulfide (ZnS), the resulting CdSe/ZnS core/shell QD possesses a stronger photoluminescence, which is particularly important for use in biological applications.⁸ Precise control over the dispersion and lateral distribution of the QDs within nanoscopic porous media provides a unique route to manipulate the optical and/or electronic properties of QDs in a very simple and controllable manner for the applications related to light emitting, optoelectronic, and sensor devices. To date, a few elegant studies have been demonstrated to disperse QDs, rather than fabricate one-dimensional nanowires of the QDs, in diblock copolymer templates via capillary force assisted deposition⁹ or electrophoretic deposition.¹⁰ However, the amount of QDs within diblock copolymer templates was not readily obtained.

Here, we study the optical properties of CdSe/ZnS core/shell QDs by directly depositing them in the host material, PAM, through dip coating. The amount of deposited QDs is

quantified by modeling the change in reflection and transmission spectra of the PAMs when one side is open and when it is freestanding (i.e., both sides are open), respectively. Filling the PAM with QDs modulates the dielectric environment of the PAM, which in turn causes shifts in spectra; the fluorescence of the QDs in PAM is retained. Such directed deposition of QDs within an array of well-ordered PAM nanopores would offer a significant advance in controlling the lateral distribution and spacing of QDs, and thus open up an avenue to manipulate optoelectronic properties of QDs in a very simple and controllable manner and to explore the feasibility of utilizing QD/PAM nanocomposites for sensor applications.

Two types of PAMs, produced by using a two-step anodization of 99.999% pure Al foil in 0.3M oxalic acid at 42 V at 0 °C for 2.5 h,¹ were used in the study. The first type was the one-side-open membrane obtained right after the second anodization. The remaining Al at the bottom of the membrane served as a reflective layer for reflection spectrum measurements. The second was a freestanding membrane (i.e., two sides open) fabricated by removing the remaining Al in saturated copper chloride (CuCl₂) solution and performing the barrier layer removal in 5 wt % phosphoric acid at 30 °C for 1 h. The PAMs were thoroughly rinsed with de-ionized water, acetone, and alcohol, and dried.

Two tri-*n*-octylphosphine oxide (TOPO) functionalized core/shell CdSe/ZnS QDs were prepared according to the well-established procedure.¹¹ The diameters of the QDs are 4.4 and 5.5 nm, respectively, as determined by transmission electron microscopy (data not shown), corresponding to the growth of two to three atomic layers of ZnS,¹² given the original CdSe diameters of 3.0 and 4.0 nm, respectively. The 4.4 nm QDs are orange emitting with maximum emission, λ_{\max} , at 598 nm; the 5.5 nm QDs are red emitting with λ_{\max} at 632 nm.

The deposition of QDs was driven by the capillary force.⁹ The PAMs were dipped into 0.5 mg/ml QD chloroform solutions for several seconds and slowly withdrawn normal to the solution surface, and then dried in air for several minutes so that the QDs were trapped within the cylindrical nanopores of the PAMs. Finally, the PAMs were immersed into fresh chloroform for ten times to exhaustively

^{a)} Author to whom correspondence should be addressed; electronic mail: zqlin@iastate.edu

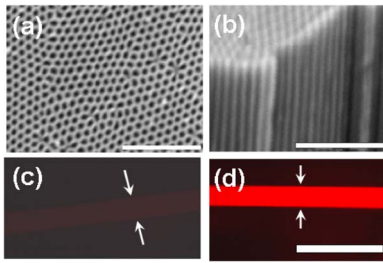


FIG. 1. (Color online) SEM images of blank PAM, fabricated by a two-step electrochemical anodization process: (a) topology and (b) cross section. Fluorescence images of the 13.22 μm thick PAM (c) before and (d) after being filled with red emitting CdSe/ZnS QDs (side view). The scale bars are 1 μm in (a) and (b), and 50 μm in (d).

rinse off the possible QDs at the PAM surface, and the washed QD-loaded PAMs were dried in air prior to the subsequent characterizations of optical properties.

Figures 1(a) and 1(b) show surface and cross-sectional scanning electron microscopy (SEM) images of a freestanding blank PAM (i.e., unfilled with QDs). The cross-sectional SEM image confirms a hexagonal array of nanoscopic porous structures with a high aspect ratio. The cylindrical nanopores are 60 nm in diameter, and the center-to-center distance λ_{C-C} between two adjacent nanopores is 110 nm. The porosity p of the PAMs is $\sim 27\%$ as determined by

$$p = \frac{2\pi}{\sqrt{3}} \left(\frac{r}{\lambda_{C-C}} \right)^2, \quad (1)$$

where r is the radius of the nanopores. This geometry provides over two orders of magnitude larger surface areas for depositions of QDs than does a single solid substrate.⁵ The lateral dimension of the PAMs used in the studies is $\sim 1 \times 1 \text{ cm}^2$.

The transmission spectra (solid curves) of freestanding PAMs before and after the deposition of CdSe/ZnS core/shell QDs with different sizes [diameter, $D=4.4 \text{ nm}$ in (a) and 5.5 nm in (b)] are shown in Fig. 2. These spectra, measured by UV-Vis spectrometer, exhibit characteristic spectral maxima and minima,⁵ and can be mathematically described using the transfer matrix formalism^{5,13} given appropriate refractive indices and incident angle (90° , i.e., normal to the membrane surface). The refractive index is a function of the membrane thickness and porosity. The excellent agreement between the simulated spectra (black dashed curves) and measured spectra (black solid curves) of the blank PAMs for the peak positions [Figs. 2(a) and 2(b)] yields the thicknesses of freestanding PAMs, which are 8.88 and 13.22 μm , respectively, using the known refractive indices and taking the porosity of blank PAM as 27% with the film thickness as the only adjustable parameter.⁵ The fluorescence images of the 13.22 μm thick PAM before and after being filled with red emitting CdSe/ZnS QDs are shown in Figs. 1(c) and 1(d). The fluorescence intensity of the PAM after the deposition of QDs is 20 folds higher than a blank counterpart under the same light intensity and exposure time. Moreover, the uniform intensity along the depth of the membrane is clearly evident [Fig. 1(d)]. Taken together, QDs were filled into the cylindrical nanopores of the PAM.

Upon the deposition of the QDs, the refractive index of the membrane changed. The effective refractive index of the QD-filled cylindrical nanopore of the PAM, $n_{\text{eff,QD}}$, can be described by the Maxwell-Garnett (MG) effective medium

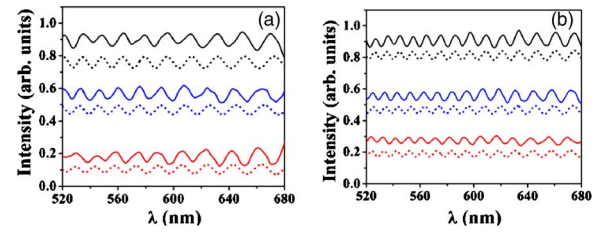


FIG. 2. (Color online) Transmission UV-Vis spectra of the freestanding PAMs with 27% porosity deposited with (a) 4.4 nm and (b) 5.5 nm CdSe/ZnS QDs. The thicknesses of the PAM in (a) and (b) are 8.88 and 13.22 μm , respectively. Black, blue, and red solid curves are the experimental spectra of the PAMs before the deposition, after the deposition, and their spectra difference, respectively. The corresponding dashed curves are the calculated spectra.

theory.^{5,14} The general relation that correlates the effective dielectric function of QDs in the nanopore, $\epsilon_{\text{eff,QD}}$, with the dielectric functions of the QDs, ϵ_{QD} , and the air, ϵ_{air} , is given by

$$\frac{\epsilon_{\text{eff,QD}} - \epsilon_{\text{air}}}{\epsilon_{\text{eff,QD}} + 2\epsilon_{\text{air}}} = f \frac{\epsilon_{\text{QD}} - \epsilon_{\text{air}}}{\epsilon_{\text{QD}} + 2\epsilon_{\text{air}}}, \quad (2)$$

where f is the volume fraction of the QDs in the nanopore.^{14,15} Since the refractive indices n and absorption coefficients k of CdSe and ZnS as a function of wavelength are known,¹⁶ the corresponding dielectric function ϵ_{QD} can be calculated based on the relation of $\epsilon = (n + ik)^2$. Here it should be noted that the refractive index of QDs is obtained as follows.¹⁷ The QDs are considered as spherical particles with a CdSe core and two coating layers (i.e., ZnS and TOPO). The volume ratios of CdSe to ZnS in the core/shell structure are 4/6 for red emitting ($D=5.5 \text{ nm}$) and 3/7 for orange emitting ($D=4.4 \text{ nm}$) QDs, respectively. The contribution from the stabilizing ligand, TOPO, is neglected in the calculation for the following reasons. First, the number of TOPO chains covering each QD was much less than 100.¹⁸ Therefore, only a very thin layer of organic compound covered the surface of the QDs. Secondly, the refractive index of TOPO is close to that of air and much smaller than those of inorganic compounds (i.e., CdSe and ZnS). Thus, the average refractive index of QDs is calculated from the volume ratio of CdSe and ZnS. The effective refractive index of the membrane, $n_{\text{eff,PAM}}$ after the loading of QDs can be written as

$$\frac{\epsilon_{\text{eff,PAM}} - \epsilon_{\text{Al}_2\text{O}_3}}{\epsilon_{\text{eff,PAM}} + 2\epsilon_{\text{Al}_2\text{O}_3}} = p \frac{\epsilon_{\text{QD/air}} - \epsilon_{\text{Al}_2\text{O}_3}}{\epsilon_{\text{QD/air}} + 2\epsilon_{\text{Al}_2\text{O}_3}}, \quad (3)$$

where $\epsilon_{\text{QD/air}} = \epsilon_{\text{eff,QD}}$ in Eq. (2), $\epsilon_{\text{Al}_2\text{O}_3}$ is the dielectric function of insulating alumina, and p is the porosity of blank PAM ($p=27\%$). Similar to the calculation of ϵ_{QD} above, the $\epsilon_{\text{Al}_2\text{O}_3}$ is obtained given the known n and k of alumina.¹⁹ Subsequently, the $n_{\text{eff,PAM}}$ obtained from $\epsilon_{\text{eff,PAM}} = (n_{\text{eff,PAM}} + ik_{\text{eff,PAM}})^2$ is substituted into the transfer matrix formalism^{5,13} with the adjustable f (i.e., the volume percentage of QDs deposited in the nanopores of the PAMs). The iterative calculations by combining Eqs. (2) and (3) are performed until best fits (blue dashed curves in Fig. 2) with experimental data (blue solid curves) are reached so that the values of f are attained.

Upon the deposition of the QDs, the transmission spectra blueshifted relative to the blank PAMs (Fig. 2). By fitting the experimental spectra (i.e., blue solid curves in Fig. 2), the uptake of QDs within the cylindrical nanopores achieved by

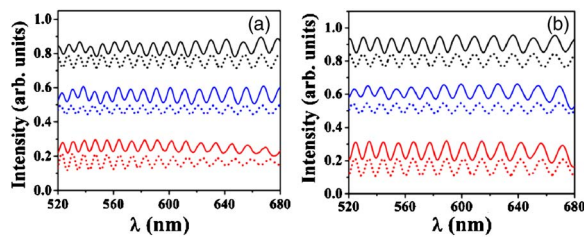


FIG. 3. (Color online) Reflection UV-Vis spectra of one-side-open PAMs with 27% porosity deposited with (a) 4.4 nm CdSe/ZnS QDs and (b) 5.5 nm CdSe/ZnS QDs. The thicknesses of the PAM in (a) and (b) are 11.44 and 9.45 μm , respectively. Black, blue, and red solid curves are the experimental spectra of the PAMs before the deposition, after the deposition, and their spectra difference, respectively. The corresponding dashed curves are the calculated spectra.

dip coating were determined to be $f=3\%$ for orange emitting QDs in the 8.8 μm thick PAM and $f=3.5\%$ for red emitting QDs in the 13.22 μm thick PAM. Thus, it is clear that the QDs only covered a very small volume of the nanopores.

Redshifts of the reflection spectra were observed upon the depositions of the QDs when one-side-open PAMs were employed (solid curves in Fig. 3). This phase difference is well known to be induced by the change of refractive index of the medium in the reflectivity measurements.⁵ The angle of incidence of the UV-Vis to the membrane surface was 22.5° in the study. A 10 nm solid Al₂O₃ barrier layer known to be formed during anodization was included in the calculation of the reflection spectra.⁵ Similar to the calculations of the transmission spectra, the thickness of the PAM and the amount f of QDs in the PAM can be determined using the transfer matrix formalism, yielding $f=2.2\%$ in the 11.44 μm thick PAM occupied by the orange emitting QDs and $f=2.8\%$ in the 9.45 μm thick PAM occupied by the red emitting QDs. It is noteworthy that the numbers of QDs loaded in one-side-open PAMs are smaller than those in the freestanding PAMs. This is due to the fact that it is much more difficult for QD chloroform solutions, driven by the capillary force, to reach the closed end of the one-side-open PAM. In contrast, the freestanding PAMs can be readily accessed by QD solutions from both sides.

After loading of the QDs within the nanopores of the PAM was confirmed, the fluorescence spectra of the PAMs before and after the deposition of the QDs were measured. The PAM exhibited blue emissions in the 400–600 nm range with a broad peak position at 420–468 nm (dashed curves in Fig. 4). These were attributed to the coactions of both the singly ionized oxygen vacancies and the luminescent centers transformed from oxalic impurities.^{15,20} The emission spectra

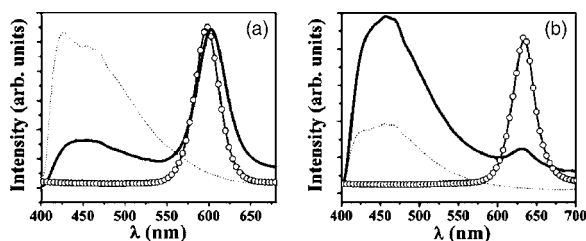


FIG. 4. Emission spectra of the freestanding PAMs before (dashed curve) and after being deposited (solid curve) with (a) 4.4 nm and (b) 5.5 nm CdSe/ZnS QDs. The corresponding emission spectra of QDs in the dry state in bulk (i.e., without confinement) are shown in open circle curves.

of the filled PAMs showed λ_{max} at 602 and 632 nm, respectively. Accordingly, it is evident that the emission of the QDs was retained. The emission of the orange emitting QDs was slightly redshifted by ~ 4 nm relative to the dry-state QDs in bulk [Fig. 4(a)]. This probably results from a slight aggregation of QDs within the nanopores. However, no shift was observed for the red emitting QDs upon confinement [Fig. 4(b)].

In conclusion, we have described the optical properties of CdSe/ZnS core/shell QDs in a hexagonal array of highly ordered cylindrical nanopores of the PAMs by a simple dip-coating method. The PAM thickness and the amount of deposited QDs were determined from both transmission and reflection spectra by modeling the changes in the UV-Vis spectra. The QD-filled PAMs were found to be highly fluorescent; their fluorescence was maintained within the cylindrical nanopores. We envision that the present study may provide some insights into optimizing nanostructured materials by spatially arranging nanoscopic elements in a well-controlled fashion for use in optoelectronic devices and biosensors.

One of the authors (J.X.) thanks the Institute for Physical Research and Technology of Iowa State University for a Catron graduate research fellowship. This work was supported by the DOE Ames Laboratory seed funding (Z.L.), the NSF-NIRT-0506832 (Z.L.), the 3 M Nontenured Faculty Award (Z.L.), and the DOE under Contract No. W-7405-ENG-82 (J.S.). The authors also thank Vladimir Tsukruk for helpful discussions.

¹H. Masuda and K. Fukuda, *Science* **268**, 1466 (1995).

²C. A. Mirkin, R. L. Letsinger, R. C. Mucic, and J. J. Storhoff, *Nature (London)* **382**, 607 (1996).

³T. Hanaoka, H. P. Kormann, M. Kroll, T. Sawitowski, and G. Schmid, *Eur. J. Inorg. Chem.* **1998**, 807 (1998).

⁴D. F. Qi, K. Kwong, K. Rademacher, M. Wolf, and J. F. Young, *Nano Lett.* **3**, 1265 (2003).

⁵S. Pan and L. J. Rothberg, *Nano Lett.* **3**, 811 (2003).

⁶V. L. Colvin, M. C. Schlamp, and A. P. Alivisatos, *Nature (London)* **370**, 354 (1994).

⁷W. U. Huynh, J. J. Dittmer, and A. P. Alivisatos, *Science* **295**, 2425 (2002).

⁸I. L. Medintz, H. T. Uyeda, E. R. Goldman, and H. Mattoussi, *Nat. Mater.* **4**, 435 (2005).

⁹M. J. Misner, H. Skaff, T. Emrick, and T. P. Russell, *Adv. Mater. (Weinheim, Ger.)* **15**, 221 (2003).

¹⁰Q. L. Zhang, T. Xu, D. Butterfield, M. J. Misner, D. Y. Ryu, T. Emrick, and T. P. Russell, *Nano Lett.* **5**, 357 (2005).

¹¹X. Peng, L. Manna, W. D. Yang, J. Wickham, E. Scher, C. Kadavanich, and A. P. Alivisatos, *Nature (London)* **404**, 59 (2000).

¹²M. A. Hines and P. Guyot-Sionnest, *J. Phys. Chem.* **100**, 468 (1996).

¹³P. Yeh, *Optical Waves in Layered Media* (Wiley-Interscience, New York, 1988).

¹⁴C. A. Foss, Jr., G. L. Hornyak, J. A. Stockert, and C. R. Martin, *J. Phys. Chem.* **98**, 2963 (1994); C. A. Foss, Jr., M. J. Tierney, and C. R. Martin, *ibid.* **96**, 9001 (1992).

¹⁵J. Hohlbein, U. Rehn, and R. B. Wehrspohn, *Phys. Status Solidi A* **201**, 803 (2004).

¹⁶E. D. Palik, *Handbook of Optical Constants of Solids* (Academic, New York, 1985); *Handbook of Optical Constants of Solids II* (Academic, New York, 1991).

¹⁷C. F. Bohren and D. R. Huffman, *Absorption and Scattering of Light by Small Particles* (Wiley-Interscience, New York, 1998).

¹⁸G. Kalyuzhny and R. W. Murray, *J. Phys. Chem. B* **109**, 7012 (2005).

¹⁹L. J. Harris, *J. Opt. Soc. Am.* **45**, 27 (1955).

²⁰W. L. Xu, M. J. Zheng, S. Wu, and W. Z. Shen, *Appl. Phys. Lett.* **85**, 4364 (2004).